Circularly Polarized Fabry Perot Cavity Antennas with Peripheral Roughness in Superstrate Unit Cells

Sagar Jain and Shobha Sundar Ram
Indraprastha Institute of Information Technology Delhi, New Delhi 110020 India
E-mail: {sagar17115,shobha}@iiitd.ac.in

***Abstract*—Fabry Perot cavity (FPC) antennas have been extensively researched and developed for their reduced fabrication complexity and cost as compared to other high gain planar antennas. Recently, the partially reflecting surfaces (PRS) of the FPC antennas have been engineered with metasurfaces with desirable electromagnetic properties in order to reduce their profile dimensions. These surfaces usually consist of an array of unit cells that are skillfully designed in order to obtain high bandwidth or desired polarization. In this paper, we have considered a unit cell design of a rectangular loop with a diagonal - with an objective of achieving circular polarization. Then we introduced a new design parameter in the form of peripheral roughness in the edge of each of the unit cells. We demonstrate that the incorporation of the new design feature in the unit cell results in an enhancement of the return loss bandwidth to 202.8 MHz (8.9%) and gain to 9.5 dBi along with a reduced axial ratio of 4.8dB.**

Keywords- Fabry Perot cavity antenna, superstrate, roughness, metasurface.

I. Introduction

The commonly used patch antenna is a low profile antenna that is easy to design and fabricate. However, the antenna is characterized by low gain and bandwidth [1]. One way to increase the gain is to use multiple patch elements configured as an antenna array with a single feed supporting a feed distribution network such as corporate feed network or a series feed network [1]. However, the major disadvantage is the increase in the aperture size of the antenna and the poor efficiency of the large and complicated feed network. Fabry Perot cavity (FPC) antennas have been explored over the last decade for communication and radar applications for their high gain, simple feed structure, ease of fabrication and small aperture size [2]–[5]. An FPC antenna consists of a primary radiator at the base of a dielectric cavity sealed with a partially reflecting surface (PRS) at the other end. Excitation from the radiator is partially reflected by the PRS back into the cavity that is backed by a ground plane on the other end. Multiple reflections within the cavity enhance the gain of the antenna. Thus FPC antennas are essentially single feed antennas without a complicated feed distribution network [4].

An FPC antenna can also be used for beamforming. In [6], the beam was steered by shifting the primary radiator from the cavity center. A compact steerable FPC antenna was proposed in [7] which consisted of a phase varying PRS placed at a distance from the patch primary radiator on a substrate backed by a ground plane. The PRS consisted of a periodic array of copper strips in the unit cell. Non-uniform spacing between the unit cells were designed to vary the reflection phase with the frequency in order to steer the antenna beam. All the FPC antennas, discussed above, are of linear polarization. In some applications involving mobile users, circular polarization is desired to eliminate the possible polarisation mismatch between the transmitted and received signals. This ensures that the receiver antenna receives maximum power from the transmitter antenna irrespective of both the antenna orientations. In other words, the need for alignment of transmitter and receiver antenna for the receiver to receive maximum power gets eliminated.

There are two methods for achieving circular polarization with an FPC antenna. The first method is to use a circularly polarized primary radiator. For example, a feed point at a particular position on an asymmetric patch could be used. However, this technique is more prone to tolerance errors and has a narrow bandwidth. Another method is to use two orthogonal feed points fed with a 90° hybrid [8], [9]. However, it introduces fabrication complexity in the feeding network leading to issues in cost and efficiency, particularly for applications in the millimeter-wave range [4]. The second method for achieving circular polarization is by using a linearly polarized primary radiator. The polarization is subsequently changed to circular by the PRS. For example, in [10], a low-profile circularly polarized FPC antenna was proposed with a linearly polarized diagonally tilted microstrip patch and integrated with the non-standard artificial magnetic conductor (AMC). An AMC is a type of engineered material which acts as a perfect magnetic conductor (PMC) over a small frequency range [11]. It usually has nearly zero reflection phase at the operating frequency. However, the non-standard AMC employed in [10] had non zero reflection phase of 45° and -45° along two orthogonal directions of the plane. The superstrate layer consisted of a unit cell array containing a square lattice with two orthogonal slots. A narrowband circularly polarized antenna using FPC configuration was proposed in [12] where a single layer polarising frequency selective surface (FSS) was placed over a linearly polarized source on a corrugated ground plane. The corrugations were introduced in the ground plane to create resonant conditions for the two orthogonal polarization components. In [13], a circularly polarized FPC antenna was designed with a metasurface as the superstrate layer. The metasurface consisted of a unit cell array where each unit cell consists of a rectangular loop with a diagonal microstrip embedded inside it. The source antenna was placed at a distance of about 1/17 λ_0 (where λ_0 is the operating wavelength in free space) from the superstrate. Both a patch and slot antenna were used in this paper as the primary radiators resulting in significant increase in return loss bandwidth and substantial improvement in the axial ratio.

In this paper, we examine a new method for improving antenna characteristics. We consider the unit cell design presented in [13] and introduce peripheral roughness to its elements. Roughness, here, refers to the serrations introduced around the periphery of the element. The size, position, distribution and the number of such serrations provide several additional degrees of freedom to the antenna designer without any significant increase in the antenna aperture size or fabrication costs. Our results show that the introduction of the roughness results in an improvement of the antenna bandwidth from 188 MHz to 203 MHz and in reducing the axial ratio from 7.6dB to 4.8dB. Our paper is organized in the following manner. In the following section, we present the design of the FPC antenna including the primary radiator, the unit cell in the superstrate and the roughness in the unit cell. In Section III, we present the simulated results of the antenna characteristics where we

978-1-7281-6813-5/20/$31.00 ©2020 IEEE

show the effect of the introduction of the roughness parameter on the unit cell elements.

II. Design of FPC antenna

The FPC antenna that we have designed consists of a patch antenna as a primary radiator. The general side view structure of the FPC antenna is shown in Fig.1.

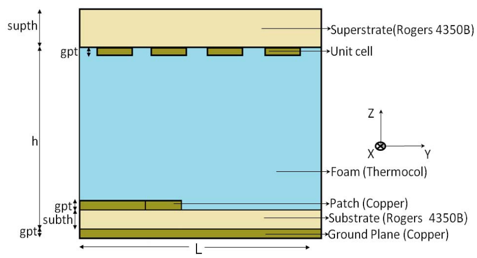

Fig. 1: Side view of proposed Fabry Perot cavity (FPC) antenna containing rectangular loop with diagonal microstrip in the unit cell placed beneath the superstrate layer. The substrate is Rogers 4350B while the unit cell elements are of copper. The foam is made of thermocol.

A. Patch antenna as primary radiator

The figure shows the bottom layer with a patch element, of thickness gpt, as the primary radiator. The patch has a single feed and is backed by a substrate layer, of thickness $subth$, followed by ground plane, also of gpt thickness. A foam of $h - subth$ thickness is mounted above the patch element and followed by the partial reflecting surface consisting of an array of metallic unit cells followed by a dielectric superstrate of $supth$ thickness. We have chosen Rogers 4350B laminate as both the substrate and the superstrate layers. The foam is made of thermocol of dielectric constant = 1.05 and provides mechanical support to the latter. We designed the simple patch at a resonant frequency of 2.45GHz. The top view of a simple patch antenna is shown in Fig.2. The length and width of the patch and the

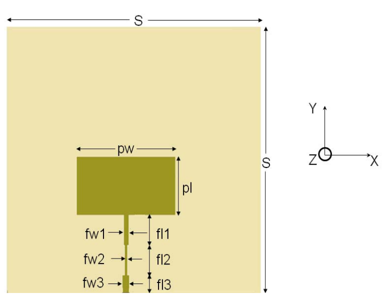

Fig. 2: A simple patch antenna on Rogers 4350B substrate of thickness $0.76mm$. The patch was designed at resonant frequency of 2.45GHz. The dimensions of the patch are $pl \times pw$. A two-stage quarter-wave transformer is employed for the patch design. The widths of the three feeds shown in the figure are $fw1$, $fw2$ and $fw3$. The lengths of the three feeds are $fl1$, $fl2$ and $fl3$.

feed were tuned individually to obtain the desired resonant frequency. A two-stage quarter-wave transformer was used to impedance match the patch to a coaxial feed of 50Ω as shown in Fig.2. The widths of the quarter wave transformer are $fw1$, $fw2$ and $fw3$ and their lengths are $fl1$, $fl2$ and $fl3$. The length and width of the patch are pl and pw, respectively. The parameters of the patch design are shown in Table I.

TABLE I: Design parameters of patch antenna

Patch Dimensions	Values(mm)
pl	33
pw	63
$fl1$	17
$fl2$	17
$fl3$	9.5
$fw1$	2.89
$fw2$	1.63
$fw3$	4.65
$subth$	0.76
gpt	0.035
S	120
L	120

B. Design of Unit Cell in Superstrate

We designed the superstrate with a 4×4 array of uniform unit cells of dimensions $ll \times lw$ as shown in Fig.3b. Each unit cell is

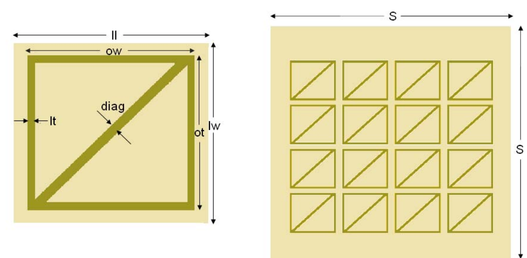

(a) (b)

Fig. 3: (a) Rectangular loop with the diagonal in the unit cell, (b) Metasurface superstrate containing 4×4 arrangement of such unit cells.

assumed to be a rectangle with one diagonal as shown in Fig.3a. We performed a parameter sweep to optimize the design parameters of the unit cell for maximum gain and bandwidth, and minimum axial ratio. The design parameters are the length and width of the rectangle ($ow \times ot$), the thickness of the sides (lt) and the thickness of the diagonal ($diag$). We also optimize the length and width of the unit cell ($ll \times lw$). An additional important design parameter is the cavity height of the FPC. Based on our simulations, the optimal design parameter values are shown in Table II.

TABLE II: Design parameters for the unit cell metasurface below the superstrate layer

Parameter	Values(mm)
ll	26.25
lw	22
h	6.05
$supth$	1.524
lt	1.05
$diag$	1.26
ow	23.1
ot	19.9

C. Design of Peripheral Roughness in the Unit Cell

The new design parameter that we propose in this paper is roughness around the periphery of the unit cell elements. We consider two cases. First, we introduce roughness to both the inner and outer peripheries of the loop and the diagonal, as shown in Fig.7a. We call this as the type-1 unit cell henceforth. In the second case, we introduce the roughness only to the inner periphery of the rectangular loop and the diagonal, as shown in Fig.7b. We refer to this unit cell design as the type-2 unit cell. In both cases, the roughness is introduced through multiple metal bricks of $0.004\lambda\,(20mil) \times 0.004\lambda\,(20mil)$ dimensions. The total number of non-overlapping bricks in the first and second cases are 375 and 207 respectively. The total number of possible brick arrangements for both cases is very large (of the order of 10^{40}). The position of the brick was varied so as to create a hundred different designs through randomization of each brick position. In other words, the brick position was randomized within a single unit cell in each iteration, and then this same design was replicated sixteen times to create the unit cell array. In this way, we generated hundred different PRS for each of the two unit cell types.

Based on the design parameters discussed in this section, all the antenna designs were realized in CST Microwave Studio. The return loss, gain and axial ratio for each of these designs were simulated and the results are presented in the following section.

III. Results

First, we demonstrate how the antenna characteristics of a simple patch antenna are improved by the introduction of a suitable superstrate layer consisting of unit cell array thereby forming an FPC structure. Fig.4 compares three antenna characteristics - return loss, gain and axial ratio - for a simple patch and for an FPC antenna with metasurface containing a rectangular loop with the diagonal (FPCMRLD) in the unit cell. As we can see, adding the superstrate layer enhanced the return loss bandwidth to 188.5MHz (8.4%). This is due to the presence of two resonant frequencies at 2.2GHz and 2.3GHz respectively whereas simple patch has a single resonant frequency at 2.45GHz.

We observe that the gain of the FPC antenna with rectangular loop and the diagonal in the unit cell is 9.4dBi at a resonant frequency of 2.3GHz whereas the simple patch has a gain of 3.4dBi at the resonant frequency of 2.45GHz. The axial ratio of FPC antenna is 7.6dB at a resonant frequency of 2.3GHz whereas that of the simple patch is 40dB. Even though the axial ratio of the FPC antenna is significantly reduced, the antenna is still linearly polarised. Hence, we consider the addition of peripheral roughness to the unit cell designs.

First, we consider the type-1 unit cell where the roughness is introduced on both the inner and outer peripheries of the loop and the diagonal in the unit cell. The roughness was incorporated in the design through two-dimensional bricks of $0.004\lambda(20mils) \times 0.004\lambda(20mils)$ dimensions and their positions were randomized as mentioned above. In Fig.5, we present histograms to show the sensitivity of the antenna characteristics to the roughness design parameters. The figure shows that the bandwidth is drastically reduced by the introduction of roughness. We also observed a slight degradation in the gain. What is encouraging, though, is that the axial ratio of the FPC antenna is reduced significantly. From the histogram, we can see that the maximum and minimum bandwidth of hundred FPC antenna with different roughened metasurface designs is 113.3MHz and 58.8MHz respectively. The maximum and minimum gain are 9.4dBi and 9dBi respectively while the maximum and minimum axial ratio are 5.4dB and 4.0dB respectively. The unit cell designs that give rise to the maximum and minimum axial ratio are shown in Fig.7a.

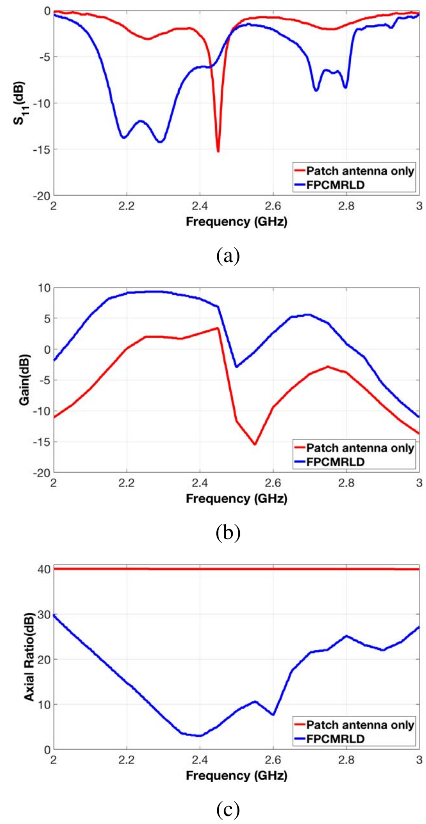

Fig. 4: Comparison of the simulation results for the simple patch antenna and FPC antenna with metasurface containing rectangular loop with the diagonal (FPCMRLD) in the unit cell: (a) Return loss, (b) Gain, (c) Axial Ratio.

Finally, we consider the type-2 unit cell with the peripheral roughness only in the inner periphery of the rectangular loop and the diagonal. As mentioned in the previous section, the dimensions of the bricks constituting the roughness were kept constant but their positions were randomly changed to obtain hundred different designs. Fig.6 shows the histograms that capture the variation of the return loss bandwidth, gain and axial ratio respectively for the different rough unit cell designs. The histograms show that the bandwidth and axial ratio of the antenna are very sensitive to the roughness. The gain, on the other hand is only moderately affected by the peripheral roughness. The maximum and minimum bandwidths are 242MHz and 178MHz respectively; the maximum and minimum gains are 9.8dBi and 9.4dBi respectively. The maximum and minimum axial ratios are 7.5dB and 4.8dB respectively. The unit cell designs that give rise to the maximum and minimum return axial ratio are shown in Fig.7b. The optimum design has a minimum axial ratio of 4.8dB, a bandwidth of 202MHz and a gain of 9.5dBi. Therefore we can see that FPC antenna with metasurface with type-2 unit cell (roughness present in the inner periphery of the rectangular loop and the diagonal) has better return loss bandwidth, gain, and reduced axial ratio as compared to that with smooth rectangular loop and the diagonal in the unit cell.

In the Table III we summarize the antenna characteristics for a simple patch antenna, the FPC antenna with a smooth unit cell superstrate, the FPC antenna with a rough unit cell with roughness

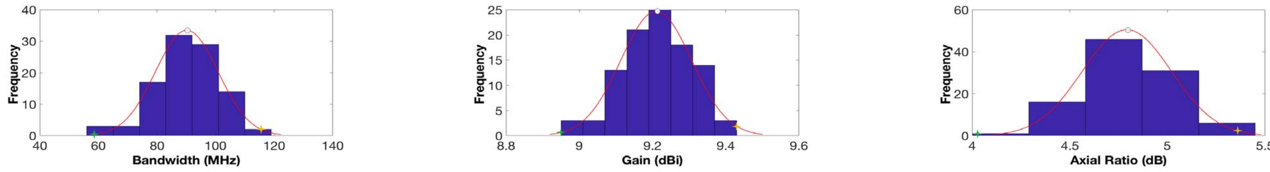

(a) (b) (c)

Fig. 5: Histogram depicting variations for hundred different designs of metasurface unit cells - with roughness present on both sides - for (a) return loss bandwidth (b) gain and (c) axial ratio. The peak of the red curve denotes the mean of the all hundred different designs of FPC antenna.

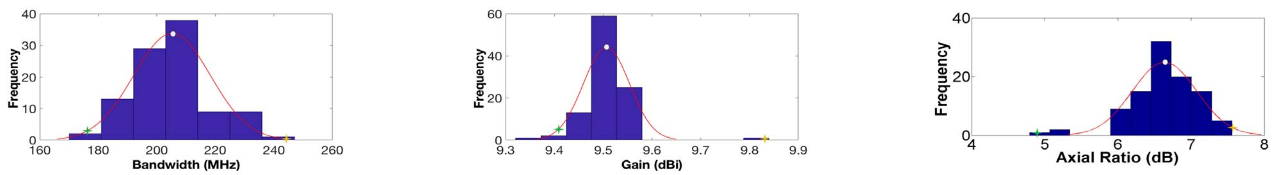

(a) (b) (c)

Fig. 6: Histogram depicting variations for hundred different designs of metasurface unit cells - with roughness present on inner periphery - for (a) return loss bandwidth, (b) gain and (c) axial ratio. The peak of red curve denotes the mean of the FPC antenna for all such hundred different designs.

TABLE III: Comparison of antenna characteristics

Antenna	Bandwidth (MHz)	Gain (dBi)	Axial Ratio (dB)
Simple patch	20	3.4	40
FPC with smooth unit cell	188.5	9.4	7.6
Proposed FPC with rough unit cell (type 1)	100.2	9.3	4
Proposed FPC with rough unit cell (type 2)	**202.8**	**9.5**	**4.8**

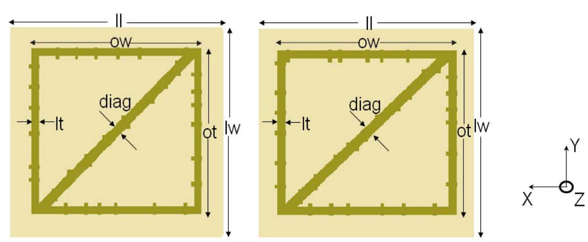

(a) Roughness on both the peripheries of the rectangular loop and the diagonal - type 1 unit cell.

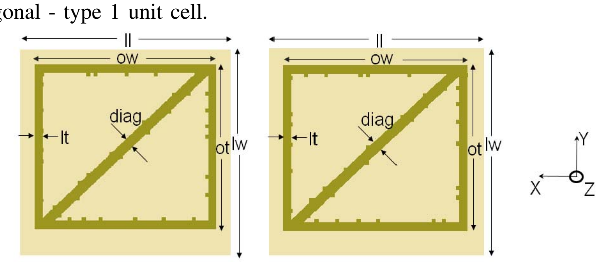

(b) Roughness along the inner periphery of the rectangular loop and the diagonal - type 2 unit cell.

Fig. 7: Unit cell designs giving rise to maximum and minimum axial ratio.

on both sides of the periphery and the optimized FPC antenna with a rough unit cell with roughness only on the inner side of the periphery. Next, we study the correlation between the antenna characteristics and the design parameters. The correlation coefficient between two data sets X and Y, is

TABLE IV: Covariance and correlation coefficient between antenna characteristics for FPC antenna with type 1 unit cell

X	Y	$Cov(X,Y)$	$\rho(X,Y)$
Bandwidth (MHz)	Axial Ratio (Linear scale)	-0.60	-0.36
Bandwidth (MHz)	Gain (Linear scale)	1.84	0.93
Gain (Linear scale)	Axial Ratio (Linear scale)	-0.01	-0.42

$$\rho(X,Y) = \frac{Cov(X,Y)}{\sqrt{Var(X)Var(Y)}}, \tag{1}$$

where $Var(X)$ and $Var(Y)$ denote the variances of data sets X and Y respectively. $Cov(X,Y)$ denotes the covariance between the data sets and is given by

$$Cov(X,Y) = E[XY] - E[X]E[Y], \tag{2}$$

where

$$E[XY] = \frac{\sum_{n=1}^{N} X_i Y_i}{N}. \tag{3}$$

Here N denotes the total number of samples in the two data sets. Table IV shows the values of covariance and correlation coefficient for the FPC antenna with the type 1 unit cell (rectangular slot with peripheral roughness on both inner and outer periphery) while Table VI shows the same for the FPC antenna with the type 2 unit cell (rectangular slot with peripheral roughness on only inner periphery).

TABLE V: Table depicting mean and variance of the antenna characteristics for FPC antenna with type 1 unit cell

	Mean	Variance
Bandwidth (MHz)	90.13	114.26
Gain (Linear scale)	8.34	0.03
Axial Ratio (Linear scale)	3.02	0.03

TABLE VI: Table depicting covariance and correlation coefficient between antenna characteristics for FPC antenna with type 2 unit cell

X	Y	$Cov(X, Y)$	$\rho(X, Y)$
Bandwidth (MHz)	Axial Ratio (Linear Scale)	-4.63	-0.72
Bandwidth (MHz)	Gain (Linear scale)	0.74	0.55
Gain (Linear Scale)	Axial Ratio (Linear scale)	-0.03	-0.53

TABLE VII: Table depicting mean and variance for different antenna characteristics for FPC antenna with type 2 unit cell

	Mean	Variance
Bandwidth (MHz)	205.17	174.04
Gain (Linear Scale)	8.93	0.01
Axial Ratio (Linear Scale)	4.66	0.24

The design objective is to obtain antennas with large bandwidth, high gain and low axial ratio. This implies that we desire a correlation coefficient close to -1 between bandwidth and axial ratio and bandwidth and gain, whereas it should be close to 1 between the bandwidth and gain. Comparing Table IV and VI, we see that the correlation coefficient is -0.72, i.e., it is closer to -1 for FPC antenna with type 2 unit cell than that for FPC antenna with type 1 unit cell. The correlation coefficient between the bandwidth and the gain is close to 1 for the latter. Since the main criteria for choosing the unit cell design is to obtain low axial ratio for achieving circular polarization, unit cells of type 2 design are preferred over unit cell of type 1 design.

IV. Conclusion

In this paper, we designed a metasurface with a unit cell array of a rectangular loop with a diagonal and roughness along the inner peripheries. The objective of the design was to obtain a circular polarized antenna without compromising bandwidth and gain. We observed that introducing the metasurface superstrate layer with rectangular loop with diagonal in the unit cell enhanced the gain and bandwidth and significantly decreased the axial ratio. Roughness in the inner periphery as opposed to both peripheries of the rectangular loop and the diagonal of the metasurface further decreased the axial ratio and improved the gain and bandwidth. We achieved a minimum axial ratio 4.8dB for a return loss bandwidth of 202.8MHz and gain of 9.5dBi.

References

[1] C. A. Balanis, *Antenna theory: analysis and design*. John wiley & sons, 2016.

[2] N. Guérin, S. Enoch, G. Tayeb, P. Sabouroux, P. Vincent, and H. Legay, "A metallic fabry-perot directive antenna," *IEEE Transactions on Antennas and Propagation*, vol. 54, no. 1, pp. 220–224, 2006.

[3] R. Gardelli, M. Albani, and F. Capolino, "Array thinning by using antennas in a fabry–perot cavity for gain enhancement," *IEEE Transactions on Antennas and Propagation*, vol. 54, no. 7, pp. 1979–1990, 2006.

[4] R. Orr, G. Goussetis, and V. Fusco, "Design method for circularly polarized fabry–perot cavity antennas," *IEEE Transactions on Antennas and Propagation*, vol. 62, no. 1, pp. 19–26, 2013.

[5] C. Lee, R. Sainati, and R. Franklin, "Parametric study of near-and far-field performance of the fabry-perot cavity antenna system," in *2016 IEEE 17th Annual Wireless and Microwave Technology Conference (WAMICON)*. IEEE, 2016, pp. 1–3.

[6] Y. Hao, A. Alomainy, and C. Parini, "Antenna-beam shaping from offset defects in uc-ebg cavities," *Microwave and Optical Technology Letters*, vol. 43, no. 2, pp. 108–112, 2004.

[7] A. Ourir, S. Burokur, and A. De Lustrac, "Phase-varying metamaterial for compact steerable directive antennas," *Electronics letters*, vol. 43, no. 9, pp. 493–494, 2007.

[8] D. Pozar, "An update on microstrip antenna theory and design including some novel feeding techniques," *IEEE Antennas and Propagation Society Newsletter*, vol. 28, no. 5, pp. 4–9, 1986.

[9] K. Carver and J. Mink, "Microstrip antenna technology," *IEEE transactions on antennas and propagation*, vol. 29, no. 1, pp. 2–24, 1981.

[10] Z.-G. Liu, Z.-X. Cao, and L.-N. Wu, "Compact low-profile circularly polarized fabry–perot resonator antenna fed by linearly polarized microstrip patch," *IEEE Antennas and Wireless Propagation Letters*, vol. 15, pp. 524–527, 2015.

[11] F. Costa, S. Genovesi, and A. Monorchio, "On the bandwidth of high-impedance frequency selective surfaces," *IEEE Antennas and Wireless Propagation Letters*, vol. 8, pp. 1341–1344, 2009.

[12] S. A. Muhammad, R. Sauleau, L. Le Coq, and H. Legay, "Self-generation of circular polarization using compact fabryperot cavity antennas," *IEEE Antennas and Wireless Propagation Letters*, vol. 10, pp. 907–910, 2011.

[13] H. Zhu, S. Cheung, K. L. Chung, and T. I. Yuk, "Linear-to-circular polarization conversion using metasurface," *IEEE Transactions on Antennas and Propagation*, vol. 61, no. 9, pp. 4615–4623, 2013.